Polymer Chemistry

Self-healing magnetic nanocomposites with robust mechanical properties and high magnetic actuation potential prepared from commodity monomers via graft-from approach

Journal:	*Polymer Chemistry*
Manuscript ID	PY-COM-11-2019-001700.R1
Article Type:	Communication
Date Submitted by the Author:	14-Jan-2020
Complete List of Authors:	Muradyan, Hurik; University of California Irvine Mozhdehi, Davoud; University of California, Chemistry Guan, Zhibin; University of California, Chemistry

Journal Name COMMUNICATION

Self-healing magnetic nanocomposites with robust mechanical properties and high magnetic actuation potential prepared from commodity monomers *via* graft-from approach

Received 00th January 20xx,
Accepted 00th January 20xx

DOI: 10.1039/x0xx00000x

Hurik Muradyan,[a] Davoud Mozhdehi [b] and Zhibin Guan[a]

Herein, we report the design, synthesis and characterization of self-healing magnetic nanocomposites prepared from readily available commodity monomers. These multi-functional materials demonstrate robust mechanical properties, with a Young's modulus of 70 MPa and over 500% extensibility. The magnetic nanocomposites also show self-healing ability, achieving 46% recovery of extensibility in 5 hours in ambient conditions while retaining high magnetic actuation with a commodity magnet.

Polymeric nanocomposites with magnetic nanoparticles (MNPs) have wide applications in stimuli-responsive materials, actuators and soft robotics. The magnetic properties of such nanocomposites allow for actuation without physical contact by using an external magnetic field.[1] Increasing the actuation potential of these materials is critical for their wide-spread use as remote actuators and is commonly achieved by increasing the fraction of MNPs.[2,3] However, the increased nanoparticle content often results in aggregation of nanoparticles and decreased mechanical performance of these materials.[4,5] Furthermore, using magnetic nanocomposites as actuators in soft robotics requires robust and durable mechanical properties.[6] Repeated motion can build up stress, generating defects that propagate and finally lead to catastrophic mechanical failure.[6,7] This is especially challenging for materials with high fractions of MNPs that are inherently more brittle.[8,9] One approach to making magnetic actuators with robust mechanical properties is to impart the materials with self-healing ability; self-healing increases the durability and functional lifetime of the material.[7,10] Intrinsically self-healing materials leverage dynamic, reversible interactions that can be accessed repeatedly upon damage to facilitate healing.[11–15] Such interactions include non-covalent interactions,[16–21] or dynamic covalent bonds,[22–26] that prevent the cascade of the damage and the delay of eventual catastrophic failure of the material.[15]

There have been significant efforts to develop magnetic nanocomposites with self-healing capabilities.[7] A common approach capitalizes on the inductive heating effect of MNPs in an alternating magnetic field.[27–36] The local heat produced from this process allows for various forms of self-healing such as melting of a thermoplastic phase,[27,28,31,35,36] facilitating bond exchange,[33,37–39] or accessing reversible reactions.[29] This method has yielded magnetic composites with good self-healing and mechanical properties; but, not all applications are amendable to applying an alternating magnetic field.

A promising alternative approach relies on the intrinsic self-healing nature of the polymeric matrices of MNP nanocomposites, without relying on the magnetic properties of the MNPs.[40–44] This approach has been demonstrated in hydrogels,[39,40,43–45] and in solid-state bulk materials;[41,46,47,42,39] however, in all these cases there is a non-covalent bond between the MNPs and the self-healing polymer. Due to the inherent attractive nature of MNPs, these approaches are susceptible to nanoparticle aggregations and macroscopic phase separation.[5] More recently, Xu et. al.[48] reported a self-healing magnetic nanocomposite using a graft-from approach such that there is a covalent linkage between the dynamic polymer and the MNPs, preventing aggregation. This represents a step forward toward the development of intrinsically self-healing bulk magnetic nanocomposites; however, the synthesis required specially designed monomers, limiting its general applicability and practical applications.

Here, we report a bulk self-healing magnetic nanocomposite using commercially available inexpensive monomers and a graft-from approach to yield stable and homogenous MNP dispersion (Scheme 1). The use of commodity monomers is expected to facilitate the translation of the material into real world applications. Our goal was to develop intrinsically self-healing magnetic nanocomposites with high actuation potential and good mechanical properties *via* a graft-from approach using readily available monomers that have not yet been investigated for self-healing behaviour. We synthesized MNPs with a narrow size distribution, then functionalized the MNPs with a radical chain-transfer agent (CTA) to allow for reversible deactivation radial polymerization from the surface. By using the graft-from approach we were able to achieve high weight percent (wt %) and homogenous dispersion of MNPs.[5] We employed an inexpensive commodity monomer, acrylamide (Am), to introduce the dynamic self-healing motif with its hydrogen-bonding amide group. To maintain polymer chain dynamics for spontaneous healing under ambient conditions, we copolymerized Am with another inexpensive commodity monomer, *n*-butyl acrylate (BA), to yield the copolymer termed BAAm. Mechanical properties and self-healing behaviour of the BAAm MNP nanocomposite were thoroughly characterized by mechanical testing. Finally, simple actuation of the magnetic

[a] *Department of Chemistry, University of California, Irvine, California 92697, United States. E-mail: zguan@uci.edu*
[b] *Department of Chemistry, Syracuse University, 1-014 Center for Science and Technology, Syracuse, NY, USA 13244.*
†Electronic Supplementary Information (ESI) available: See DOI: 10.1039/x0xx00000x

nanocomposite was demonstrated by remote actuation using a commodity external magnet.

Specifically, we first synthesized MNPs *via* a two-step thermal decomposition method to yield iron oxide nanoparticles with narrow size distribution.[49] To obtain particles we first generated an iron-oleate precursor that was characterized by differential scanning calorimetry (DSC) (Fig. S1).[50] In the second step, thermal decomposition of the precursor yielded iron oxide nanoparticles with a diameter of 21.5±1.9 nm as determined by transmission electron microscopy (TEM) (Fig. 1a). The quality of the crystalline nature of iron oxide nanoparticles was evident by the lattice fringes seen in the fast Fourier transform of the high-resolution TEM image (Fig. S2). We also characterized the surface chemistry of the MNPs *via* attenuated total reflectance (ATR) Fourier transform infrared (FTIR) spectroscopy. The two signals at 1450 and 1375 cm^{-1}, as indicated by red arrows in Fig. 1b, are characteristic of coordinated asymmetric and symmetric

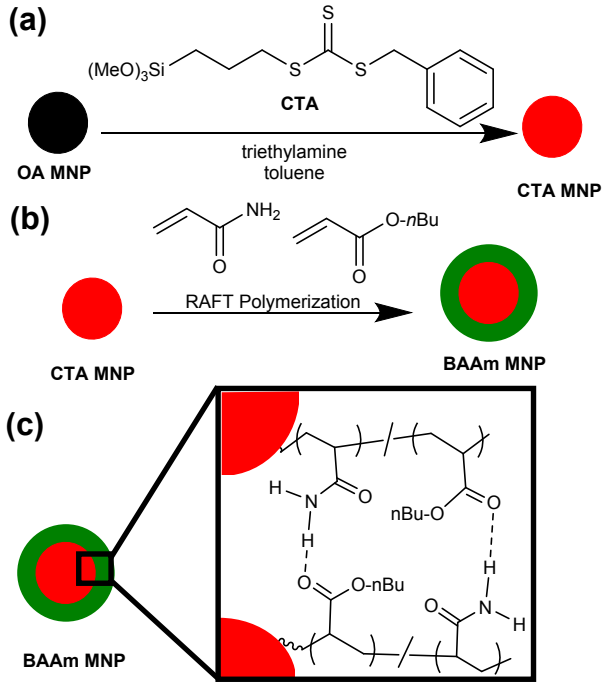

Scheme 1 Design and synthesis of magnetic nanoparticles (MNPs) grafted with acrylamide (Am) and *n*-butyl acrylate (BA) copolymers. (a) Functionalization of oleic acid (OA) MNPs with a chain-transfer agent (CTA) to yield CTA MNPs. The CTA was synthesized in one step from 3-mercaptopropyltrimethoxysilane (b) Synthesis of BAAm copolymer functionalized MNP. (c) Hydrogen bonding between Am and BA are shown as representative examples. There is also hydrogen-bonding between Am and Am monomeric units.

carboxylates stretches, which appear at a lower frequency as compared an unbound carboxylic acid that would display a signal at 1700 cm^{-1}, demonstrating the bond formation between the oleate ligand and the surface of the oleic acid (OA) MNPs.[51,52]

Next, the OA MNPs were functionalized with a radical chain-transfer agent (CTA) to facilitate polymerization from the surface. A trimethoxy-containing CTA was synthesized in one step (Scheme S1) and characterized by 1H NMR spectroscopy (Fig. S3).[53] Next the particles were modified with the CTA *via* a base-catalyzed ligand exchange that results in the covalent attachment of the CTA *via* a Fe-O-Si linkages.[54,55] The surface chemistry of the resulting particles, termed CTA MNPs, was characterized *via* ATR FTIR spectroscopy, which revealed the emergence of new vibrational stretches that corresponds to the CTA (Fig. 1b, full range FTIR spectra in Fig. S5). The characteristic peaks that confirmed successful ligand exchange include trithiocarbonate stretches from 1450-1490 cm^{-1} marked with blue double headed arrows, and siloxane stretches from 1000-1100 cm^{-1} (Fig. 1b, blue and black curves).[56–58] Surface functionalization of CTA MNPs was also supported by thermogravimetric analysis (TGA) (Fig. 1c, red and black curves), which show an increase in volatile organic content from 7 to 25 wt % after functionalization with the CTA indicating successful functionalization (Table S1). The increase in organic content upon functionalization with a lower molecular weight ligand is attributed to a higher density of the CTA as compared to the oleate ligand. The higher density of CTA (4.6 mmole/g) is ascribed to the facile base-catalyzed condensation of alkoxysilanes generating multi-layer siloxane shell, commonly seen in literature. [59–61]

The CTA MNPs were then subject to surface-initiated reversible addition-fragmentation chain transfer (si-RAFT) [62–65] polymerization with the comonomers acrylamide (Am) and *n*-butyl acrylate (BA), yielding MNPs grafted with the BAAm copolymer. The feed ratio of Am to BA was chosen to be 30 mole % Am and 70 mole % BA to maintain a relatively high concentration of dynamic hydrogen-bonding motifs while maintaining the sufficient polymer chain dynamics (owing to the lower glass transition temperature of BA).[66] The polymerization was monitored by ^{1}H NMR spectroscopy using mesitylene as an internal standard to ensure percent conversion was less than 50%. A range of composites with varying amounts of polymer were synthesized by quenching the polymerization at different time points. The composites are referred to as BAAm-MNP-XX, where XX is the weight percent of volatile organic components as determined by thermogravimetric analysis including XX = 75, 81, 85, 86 (Table S1). After si-RAFT copolymerization the BAAm-MNPs were purified from unreacted monomer *via* precipitation prior to characterization. BAAm-MNP nanocomposites were characterized by TGA, revealing an increase in the organic content from 25 wt % in the CTA-MNPs (Fig. 1c, black curve) to 75-86 wt %, as seen in Table S1, for the range of BAAM-MNP nanocomposites synthesized (TGA characterization of all composites in Fig. S4). FTIR spectroscopy further supports the functionalization of BAAm copolymer on the surface of the nanoparticles as evident in the signals at 1724 and 1672 cm^{-1}, marked with two green arrows in Fig. 1b, which are characteristic of carbonyl stretches for BA and Am, respectively (Fig. 1b, green curve).[58] Due to the graft-from approach, it is possible to achieve large wt % of the inorganic phase while maintaining homogeneity of nanoparticle distribution. This is evident in the TEM characterization of BAAm MNPs that show the nanoparticles to be colloidally stable and well dispersed from one another (Fig. 2a). Homogenous dispersion of the MNP is attributed to the graft-from approach that results in a

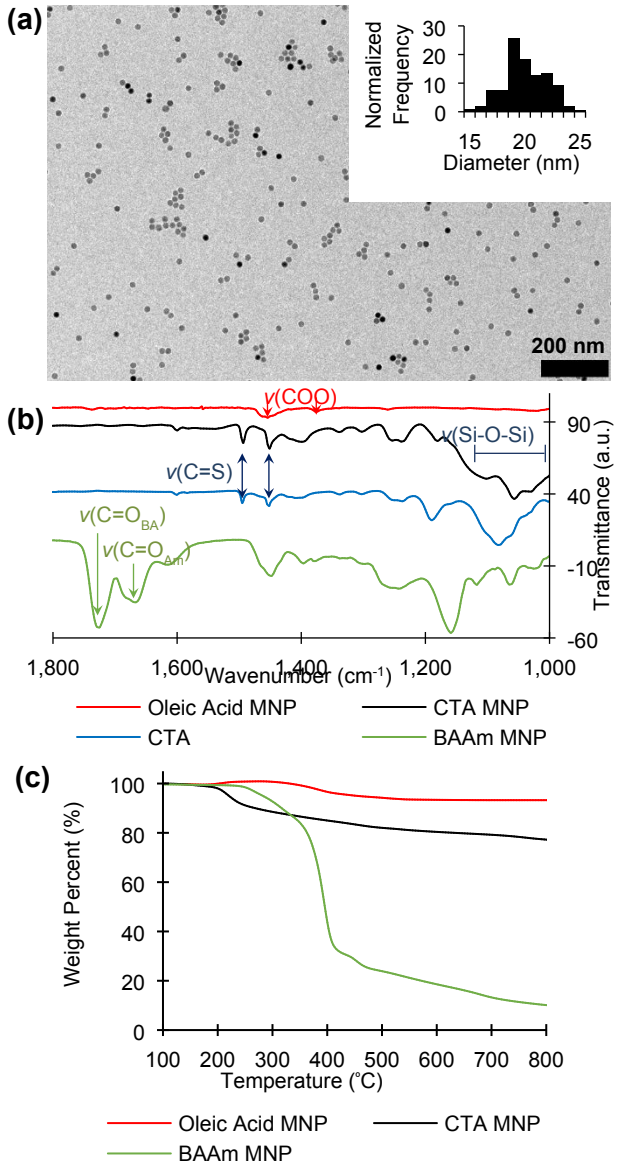

Fig. 1 (a) Transmission electron micrograph of oleic acid MNPs. Inset showing size distribution in terms of normalized frequency with an average diameter of 21.5±1.9 nm. Scale bar is 200 nm. (b) Attenuated total reflectance Fourier transform infrared spectroscopy of oleic acid MNP (red), CTA MNP (black), free CTA (blue), and BAAm-MNP-75 (green) (c) Thermogravimetric analysis of oleic acid MNP (red), CTA MNP (black), and BAAm MNP-75 (green).

covalent linkage between the dynamic polymer and the MNPs, which overcomes the phase separation issue that is common when physically blending incompatible materials.

Next the mechanical properties of the nanocomposites with varying content of MNPs were characterized by uniaxial mechanical testing (Fig. 2b & Table S1). Stress-strain curves showed clear differences in the mechanical properties that correlate with the relative polymeric content (Fig. 2c). All samples exhibited high extensibility from 540 % for BAAm-MNP-75 to 1200% for BAAm-MNP-86, respectively (Fig. 2b, black and green curves). There is a clear trend that the extensibility increases with increased weight percent organic content, owing to the increase polymer content. Additionally, the toughness nearly doubles from 28 to 52 MJ/m^3 upon increasing the weight percent from 75 to 86 (Table S1). As expected, increasing the fraction of flexible and dissipative polymer chains endows the nanocomposite with higher extensibility and toughness. The reinforcing effects of the MNPs to the nanocomposite mechanical properties can be clearly seen in comparison to a control BAAm polymer without MNP (Fig. S6). The stress at break increases from 0.8 MPa for the control sample to 6.9 MPa for the BAAm-MNP-75 sample, demonstrating an eight-fold increase, while the extensibility for the BAAm-MNP-75 remains high at 540 % (Table S1). The BAAm-MNP-75 sample also exhibits a high Young's modulus of 70 MPa, significantly higher than the control which had a Young's modulus of 12 MPa (Table S1). This represents a significant improvement of mechanical properties (2-fold in modulus and 7-fold in extensibility) for intrinsically self-healing magnetic composites that self-heal at ambient conditions.

After thorough molecular, mechanical, and morphological characterization, we set to investigate the self-healing behaviour of the BAAm-MNP nanocomposites. Polymers with hydrogen bonding capabilities has been previously shown to yield robust self-healing dynamic materials.[17,18] Here, we capitalized on the dynamic hydrogen bonds between the commodity monomers, Am and BA, to allow for facile recovery of mechanical properties after incurring damage. The self-healing capabilities are tested by introducing a cut through 50% of the width of a sample, then pressing the cut interfaces together and allowing for healing for desired duration. The self-healing efficiency was quantified by uniaxial mechanical testing in comparison to pristine, uncut sample subject to the same conditions (Fig. 2d). BAAm-MNP-33 recovered 75% of its original extensibility when healed at 80 °C for 5 h under reduced pressure (Fig. S8 and Table S5). In more application relevant conditions, the BAAm-MNP-85 sample recovered 41% of the extensibility when healed at ambient conditions of 30 °C for 2 h (Fig. S7 & Table S3). It is expected that the self-healing of composites with lower amounts of polymeric material, such as in BAAm-MNP-33, to be more challenging. For this reason, the healing of BAAm-MNP-33 was extended to 5 h at 30 °C, after which 46% of the extensibility was recovered (Fig. 2d & Table S2). The observed self-healing efficiency is presumably due to the formation of new hydrogen bonds between BAAm grafts on MNPs at the cut interface (Scheme 1c).

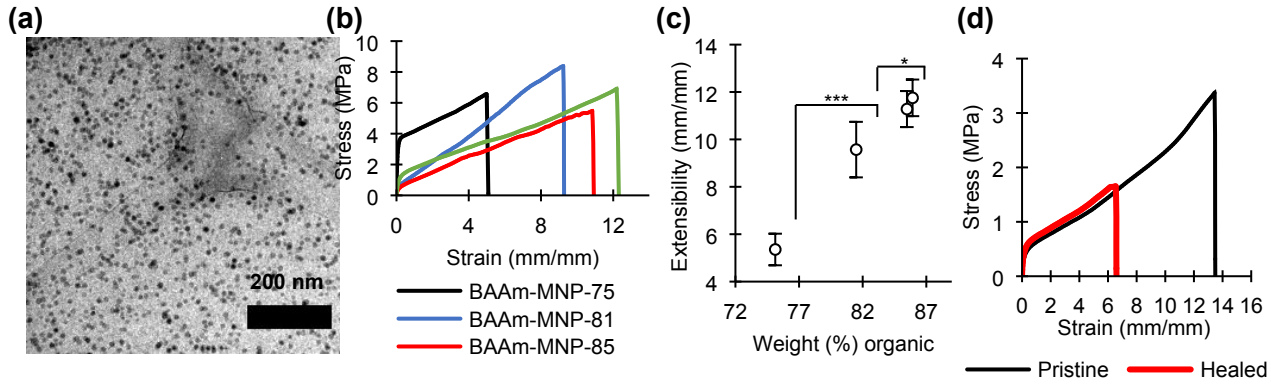

Fig. 2 (a) Transmission electron micrograph of BAAm MNP composite, scale bar 200 nm. (b) Uniaxial mechanical testing strained at 100 mm/min of representative composites. (c) Analysis of extensibility with regards to weight percent organic material. Error bars represent standard deviation from minimum of three samples. (d) Representative stress-strain curves of mechanical testing of BAAm-MNP-75 pristine and healed samples. Healing was carried out for 5 h at 30 °C (strained at 100 mm/min).

Finally, we demonstrated the potential of using the BAAm-MNP nanocomposites in practical actuation using an external magnetic source. To achieve high magnetic actuation there must be sufficiently high MNP loading. Owing to the graft-from approach, we can incorporate 25 wt % inorganic material in BAAm-MNP-75, which allowed for actuation using a commodity neodymium magnetic with a 54 kg pull force. This was demonstrated by affixing one side of a dog-bone shaped BAAm-MNP-75 sample, while bringing the magnet towards the other end of the sample, as seen in Fig. 3. The magnet was moved downwards to the sample until actuation started when the magnetic was 2 cm away (Fig. 3d&e). The nanocomposite was then actuated in the opposite direction by changing the location of the magnet, (Fig. 3f-h). Upon removal of the magnetic field the composite returned to an equilibrium position (Fig. 3i). This simple experiment demonstrates that this nanocomposite allows for facile and rapid actuation in addition of self-healing in ambient conditions, making these promising for multifunctional materials for applications as magnetic actuators.

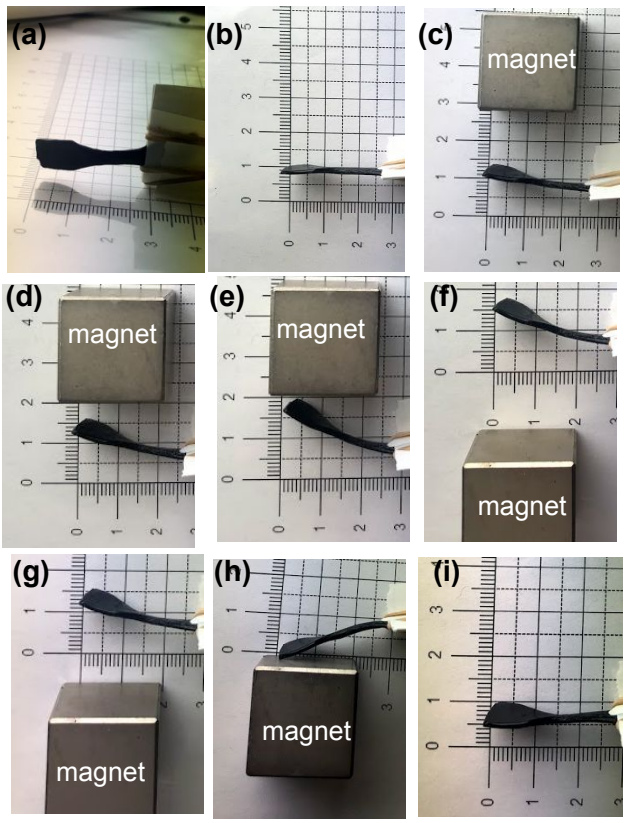

Fig. 3 Actuation of BAAm-MNP-75 sample using 2.54 cm^3 neodymium magnet (54 kg pull force). Grid in background is for measuring distance. A dog-bone sample was affixed in position in (a) a parallel view and (b) perpendicular view. (c) Magnet was placed on the 3 cm mark and (d) moved to the 2 cm mark where actuation starts and (e) finishes in less than 30 seconds. (f) Magnet was placed to the opposite side and (g) moved closer by 0.5 cm (h), then by 1 cm where actuation occurred. (i) Finally, the magnet was removed from area and the sample resumed to its original position.

Conclusions

Here we demonstrated the use of a graft-from polymerization approach to generate MNPs functionalized with an intrinsically self-healing polymer matrix that is composed of readily available inexpensive monomers. The two notable features of this work include the use of inexpensive commodity monomers which should facilitate the translation into practical applications, and the improved mechanical properties. The magnetic nanocomposite exhibits a high Young's modulus of 70 MPa and excellent extensibility of over 500% while retaining the ability to self-heal in ambient conditions. By using readily available monomers, i.e., acrylamide and *n*-butyl acrylate, the nanocomposite can self-heal mechanical damage with ~ 50% efficiency in as short as 2 hours in ambient conditions. This work contributes to the field of magnetic nanocomposites by using commodity monomers to achieve a self-healing material with excellent mechanical properties and high actuation potential, opening many applications that benefit from robust materials with prolonged lifetimes including such as remote actuation, artificial muscles and soft robotics.

Conflicts of interest

"There are no conflicts to declare".

ACKNOWLEDGMENT

This work was supported by the U.S. Department of Energy, Division of Materials Sciences, under Award DE-FG02-04ER46162. Transmission electron microscopy experiments were performed at the UC Irvine Materials Research Institute (IMRI). We acknowledge the Laser Spectroscopy Labs (LSL) at UC Irvine for the attenuated total reflectance Fourier transform infrared spectroscopy experiments.

References

1 B. Gong, A. R. Sanford and J. S. Ferguson, *Oligomers - Polymer Composites - Molecular Imprinting*, Springer, Berlin Heidelberg, 2007, 137–189.
2 M. Zrínyi and D. Szabó, *Electro-Rheol. Fluids and Magn. -Rheol. Suspensions, Proc. Int. Conf., 7th*, 2000, **15**, 11–17.
3 R. Fuhrer, E. K. Athanassiou, N. A. Luechinger and W. J. Stark, *Small*, 2009, **5**, 383–388.
4 D. W. Schaefer and R. S. Justice, *Macromolecules*, 2007, **40**, 8501–8517.
5 S. K. Kumar, N. Jouault, B. Benicewicz and T. Neely, *Macromolecules*, 2013, **46**, 3199–3214.
6 L. Ionov, *Langmuir*, 2015, **31**, 5015–5024.
7 T.-P. Huynh, P. Sonar and H. Haick, *Adv. Mater.*, 2017, **29**, DOI: 10.1002/adma.201604973.
8 J. Jordan, K. I. Jacob, R. Tannenbaum, M. A. Sharaf and I. Jasiuk, *Mater. Sci. Eng. A*, 2005, **393**, 1–11.
9 A. S. Ahmed and R. V. Ramanujan, *Macromolecular Chemistry and Physics*, 2015, **216**, 1594–1602.
10 Y. Yang and M. W. Urban, *Chem. Soc. Rev.*, 2013, **42**, 7446–7467.
11 B. J. Blaiszik, S. L. B. Kramer, S. C. Olugebefola, J. S. Moore, N. R. Sottos and S. R. White, *Ann. Rev. Mater. Res.*, 2010, **40**, 179–211.
12 S. D. Bergman and F. Wudl, *J. Mater. Chem.*, 2007, **18**, 41–62.
13 N. Zhong and W. Post, *Composites Part A,* 2015, **69**, 226–239.
14 C. E. Diesendruck, N. R. Sottos, J. S. Moore and S. R. White, *Angew. Chem. Int. Edit.*, 2015, **54**, 10428–10447.
15 N. Roy, B. Bruchmann and J.-M. Lehn, *Chem. Soc. Rev.*, 2015, **44**, 3786–3807.
16 D. Mozhdehi, S. Ayala, O. R. Cromwell and Z. Guan, *J. Am. Chem. Soc.*, 2014, **136**, 16128–16131.
17 Y. Chen, A. M. Kushner, G. A. Williams and Z. Guan, *Nat. Chem.*, 2012, **4**, 467–472.
18 P. Cordier, F. Tournilhac, C. Soulié-Ziakovic and L. Leibler, *Nature*, 2008, **451**, 977–980.
19 S. Burattini, H. M. Colquhoun, J. D. Fox, D. Friedmann, B. W. Greenland, P. J. F. Harris, W. Hayes, M. E. Mackay and S. J. Rowan, *Chem. Comm.*, 2009, **0**, 6717–6719.
20 M. Burnworth, L. Tang, J. R. Kumpfer, A. J. Duncan, F. L. Beyer, G. L. Fiore, S. J. Rowan and C. Weder, *Nature*, 2011, **472**, 334–337.
21 B. C.-K. Tee, C. Wang, R. Allen and Z. Bao, *Nature Nanotechnol.*, 2012, **7**, 825–832.
22 X. Chen, M. A. Dam, K. Ono, A. Mal, H. Shen, S. R. Nutt, K. Sheran and F. Wudl, *Science*, 2002, **295**, 1698–1702.
23 C.-M. Chung, Y.-S. Roh, S.-Y. Cho and J.-G. Kim, *Chem. Mater.*, 2004, **16**, 3982–3984.
24 M. Capelot, D. Montarnal, F. Tournilhac and L. Leibler, *J. Am. Chem. Soc.*, 2012, **134**, 7664–7667.
25 Y. Amamoto, J. Kamada, H. Otsuka, A. Takahara and K. Matyjaszewski, *Angew. Chem. Int. Edit.,* 2011, **50**, 1660–1663.
26 K. Imato, M. Nishihara, T. Kanehara, Y. Amamoto, A. Takahara and H. Otsuka, *Angew. Chem. Int. Edit.,* 2012, **51**, 1138–1142.
27 Y. Yang, J. He, Q. Li, L. Gao, J. Hu, R. Zeng, J. Qin, S. X. Wang and Q. Wang, *Nature Nanotechnol.*, 2019, **14**, 151.
28 A. S. Ahmed and R. V. Ramanujan, *Sci. Rep.,* 2015, **5**, DOI: 10.1038/srep13773.
29 B. J. Adzima, C. J. Kloxin and C. N. Bowman, *Adv. Mater.*, **22**, 2784–2787.
30 V. Q. Nguyen, A. S. Ahmed and R. V. Ramanujan, *Adv. Mater.*, 2012, **24**, 4041–4054.
31 M. Yoonessi, B. A. Lerch, J. A. Peck, R. B. Rogers, F. J. Solá-Lopez and M. A. Meador, *ACS Appl. Mater. Inter.*, 2015, **7**, 16932–16937.
32 A. S. Ahmed and R. V. Ramanujan, *J. Mater. Res.*, 2015, **30**, 946–958.
33 W. Post, R. K. Bose, S. J. García and S. Van der Zwaag, *Polymers*, 2016, **8**, DOI: 10.3390/polym8120436.
34 T. Duenas, A. Enke, K. Chai, M. Castellucci, V. B. Sundaresan, F. Wudl, E. B. Murphy, A. Mal, J. R. Alexandar, A. Corder and T. K. Ooi, *Smart Coatings III,* American Chemical Society, 2010, **1050**, 45–60.
35 C. C. Corten and M. W. Urban, *Adv. Mater.*, 2009, **21**, 5011–5015.
36 J. Huang, L. Cao, D. Yuan and Y. Chen, *ACS Appl. Mater. Inter.*, 2018, **10**, 40996–41002.
37 N. Hohlbein, A. Shaaban and A. M. Schmidt, *Polymer*, 2015, **69**, 301–309.
38 E. Ogliani, L. Yu, I. Javakhishvili and A. L. Skov, *RSC Adv.*, 2018, **8**, 8285–8291.
39 L. Du, Z.-Y. Xu, C.-J. Fan, G. Xiang, K.-K. Yang and Y.-Z. Wang, *Macromolecules*, 2018, **51**, 705–715.

40 K. Liu, X. Pan, L. Chen, L. Huang, Y. Ni, J. Liu, S. Cao and H. Wang, *ACS Sustain. Chem. Eng.*, 2018, **6**, 6395–6403.
41 X. Q. Feng, G. Z. Zhang, Q. M. Bai, H. Y. Jiang, B. Xu and H. J. Li, *Macromol. Mater. Eng.*, 2016, **301**, 125–132.
42 Y.-M. Wang, M. Pan, X.-Y. Liang, B.-J. Li and S. Zhang, *Macromol. Rapid Comm.*, 2017, **38**, 1700447.
43 Y. Zhang, B. Yang, X. Zhang, L. Xu, L. Tao, S. Li and Y. Wei, *Chem. Commun.*, 2012, **48**, 9305–9307.
44 C. Yu, C.-F. Wang and S. Chen, *Adv. Funct. Mater.*, 2014, **24**, 1235–1242.
45 Q. Li, D. G. Barrett, P. B. Messersmith and N. Holten-Andersen, *ACS Nano*, 2016, **10**, 1317–1324.
46 S. Schäfer and G. Kickelbick, *ACS Appl. Nano Mater.*, 2018, **1**, 2640–2652.
47 W. Li, G. Wu, J. Tan, Y. Zhu, X. Yu, Y. Lei, G. Sun and B. You, *J. Mater. Sci.*, 2019, **54**, 7702–7718.
48 S. Xu, B. Zhao, M. Adeel, H. Mei, L. Li and S. Zheng, *Polymer*, 2019, **172**, 404–414.
49 J. Park, K. An, Y. Hwang, J.-G. Park, H.-J. Noh, J.-Y. Kim, J.-H. Park, N.-M. Hwang and T. Hyeon, *Nat. Mater.*, 2004, **3**, 891–895.
50 L. M. Bronstein, X. Huang, J. Retrum, A. Schmucker, M. Pink, B. D. Stein and B. Dragnea, *Chem. Mater.*, 2007, **19**, 3624–3632.
51 G. B. Deacon and R. J. Phillips, *Coordination Chem. Rev.*, 1980, **33**, 227–250.
52 S. M. Gravano, R. Dumas, K. Liu and T. E. Patten, *J. Polym. Sci. Pol. Chem.*, 2005, **43**, 3675–3688.
53 Y. Zhao and S. Perrier, *Macromolecules*, 2007, **40**, 9116–9124.
54 E. Marutani, S. Yamamoto, T. Ninjbadgar, Y. Tsujii, T. Fukuda and M. Takano, *Polymer*, 2004, **45**, 2231–2235.
55 Y. Sun, X. Ding, Z. Zheng, X. Cheng, X. Hu and Y. Peng, *Eur. Polym. J.*, 2007, **43**, 762–772.
56 L. D. White and C. P. Tripp, *J. Colloid Interf. Sci.*, 2000, **232**, 400–407.
57 K. Skrabania, A. Miasnikova, A. M. Bivigou-Koumba, D. Zehm and A. Laschewsky, *Polym. Chem.*, 2011, **2**, 2074–2083.
58 A. J. Gordon and R. A. Ford, *Chemist's Companion - A Handbook of Practical Data, Techniques, and References,* John Wiley & Sons, Inc. USA, 1972.
59 J. D. Miller and Hatsuo. Ishida, *Langmuir*, 1986, **2**, 127–131.
60 R. Rotzoll, D. H. Nguyen and P. Vana, *Macromol. Symp.*, 2009, **275–276**, 1–12.
61 R. A. Bini, R. F. C. Marques, F. J. Santos, J. A. Chaker and M. Jafelicci, *J. Magn. Magn. Mater.*, 2012, **324**, 534–539.
62 J. Chiefari, Y. K. (Bill) Chong, F. Ercole, J. Krstina, J. Jeffery, T. P. T. Le, R. T. A. Mayadunne, G. F. Meijs, C. L. Moad, G. Moad, E. Rizzardo and S. H. Thang, *Macromolecules*, 1998, **31**, 5559–5562.
63 S. Edmondson, V. L. Osborne and W. T. S. Huck, *Chem. Soc. Rev.*, 2004, **33**, 14–22.
64 Y. Tsujii, M. Ejaz, K. Sato, A. Goto and T. Fukuda, *Macromolecules*, 2001, **34**, 8872–8878.
65 G. Moad, E. Rizzardo and S. H. Thang, *Aust. J. Chem.*, 2005, **58**, 379–410.
66 J. Brandrup and E. H. Immergut, *Polymer Handbook,* John Wiley & Sons, USA, 3, 1989, 277–277.

TOC